

During this operation, a commercial controller (NI-PAC) and a 24-bit RTD module with noise level

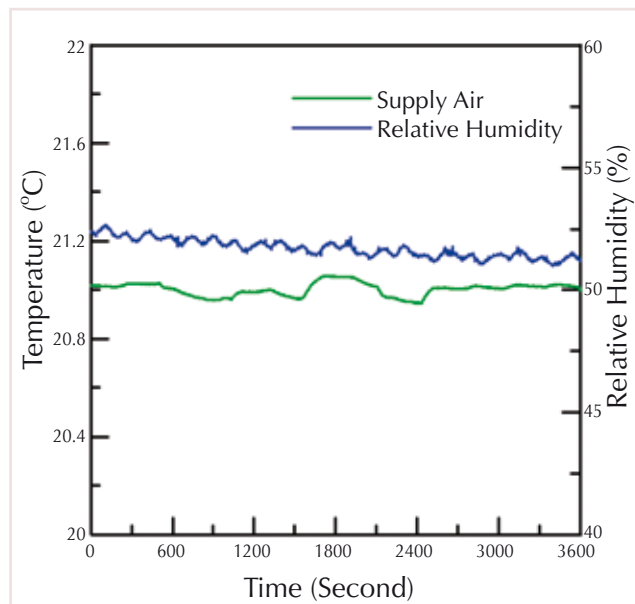


Fig. 6: Trends of temperature of supply air and relative humidity after activation of the run-around mode.

0.003 °C were used for the precise control operation. PID and fuzzy control schemes were implemented for this system. To control the humidity, the air flow via the cooling coil was controlled based on the temperature of the dew point. The supply air via the heating coil was well controlled within  $\pm 0.05$  °C through the feedback of the outlet temperature behind the heating coil. The return air was controlled based on the inlet air temperature by adjusting the fan speed to maintain the room temperature to have a constant gradient for the effect of thermal expansion of the equipment. The flow of water in the run-around system has also been adjusted by the pump speed with an inverter to distribute the thermal energy among four coils.

#### References

1. Z. D. Tsai, W. S. Chan, J. C. Chang, C. S. Chen, Y. C. Chung, C. W. Hsu, and C. Y. Liu, IPAC 2012, 2603 (2012).
2. C. W. Hsu, Z. D. Tsai, C. Y. Liu, Y. C. Chung, J. C. Chang, L. B. Zhou, and M. C. Li, "Analysis of Saving Energy for High Precision Temperature Control Air-Conditioning System", 2013 GETA, Green Technology Engineering Application Conference (2013).

## Highly Efficient Beamline and Spectrometer for Inelastic Soft X-ray Scattering at High Resolution

*This report features the work of Chia-Hung Lai and his co-workers published in J. Synchrotron Rad. 21, 325 (2014).*

Resonant inelastic soft X-ray scattering (RIXS) techniques have been developed to study the electronic and magnetic properties of strongly correlated electron materials such as transition-metal oxides. L-edge RIXS has proved effective in detecting charge, orbital and magnetic excitations. A RIXS experiment to fulfil the high resolution to study these excitations requires, however, photons of great brilliance and a highly efficient monochromator or spectrometer. Here, we report on the design, construction and commissioning results of a beamline and spectrometer for RIXS at high resolution.

Fung *et al.*<sup>1</sup> proposed a novel design for a RIXS setup comprising two bendable gratings, termed an active-grating monochromator (AGM) or active-grat-

ing spectrometer (AGS), to enhance the efficiency of measuring the inelastically scattered X-rays through an increased bandwidth of incident photons, but without smearing the energy resolution. The design of our AGM and AGS is based on the energy-compensation principle of grating dispersion. In adopting this concept, we employed two bendable gratings with varied line spacing (VLS) in the AGM-AGS design for these advantages: an active grating can vary the surface profile to match the desired energy setting and to focus the incident and scattered X-rays onto the sample and detector, respectively; a VLS grating design provides flexible parameters of the ruling density of the grating to cancel the coma abbreviation and asymmetry of the spectral line shape.

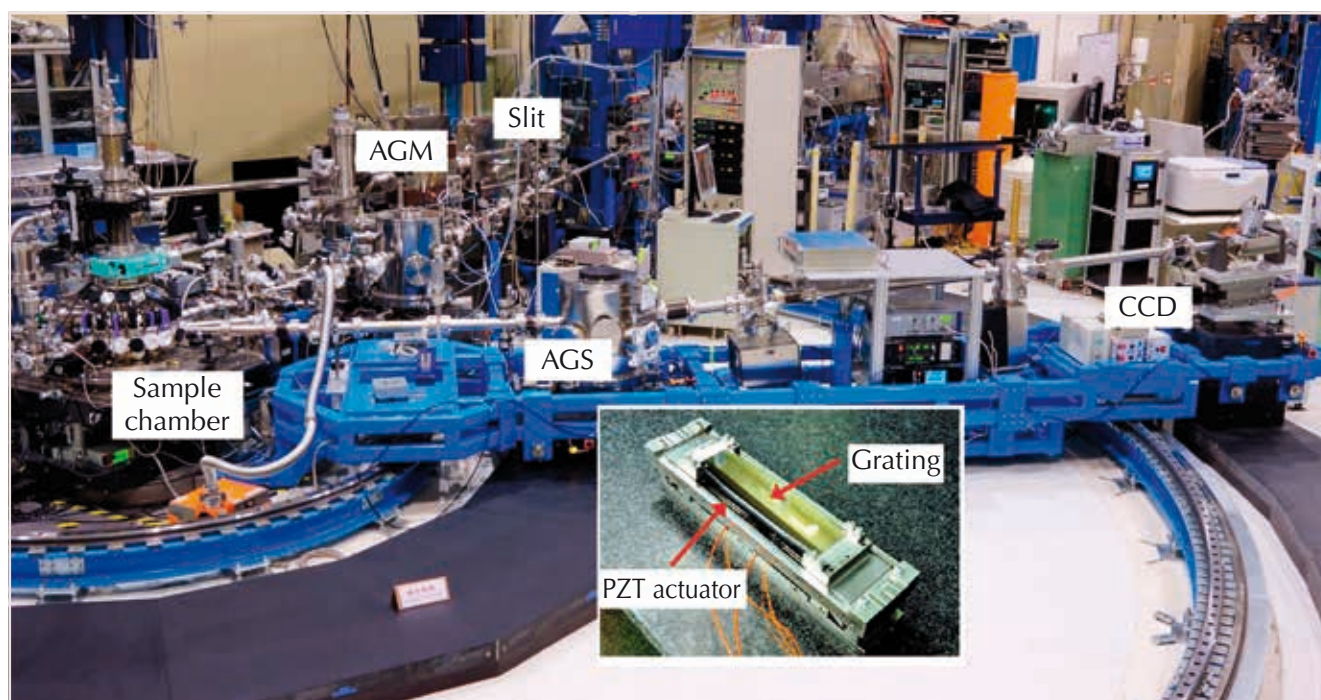


**Fig. 1:** Photographs of the AGM-AGS beamline and spectrometer installed at BL05A1 of TLS. The base granite blocks of the AGS grating and the CCD are separately placed on two granite platforms. Through an air cushion mechanism, the AGS can swing about a vertical axis at the sample position; the gap between the movable granite and the fixed granite platform is about 30  $\mu\text{m}$ . The rotation range is from 0° to 144°. Inset: photograph of the active grating; the assembly includes a Si plane grating, a bender and two high-voltage piezoelectric actuators.

To test the energy-compensation principle for RIXS experiments, we constructed an AGM-AGS setup using a side branch of beamline 05 of Taiwan Light Source (TLS). **Figure 1** shows a photograph of the test AGM-AGS beamline and spectrometer. An active grating is a key component of the AGS-AGS design. The inset of **Fig. 1** shows the active grating. A mechanical bender of clamping type was designed and fabricated to achieve a polynomial surface of the grating. The grating assembly includes three major components: a plane grating, a bender and two piezo actuators. The plane grating is made of a Si substrate coated with Au; the thickness of the substrate is 10 mm and the slope error is 0.25  $\mu\text{rad}$ . The grating was joined to a flexure-hinge bender with six screws on both sides, allowing the plane grating to be bent to a surface profile of a third-order polynomial with a radius down to 35 m. The bender was shaped with electric discharge machining to ensure that the central point of the grating surface is stationary within a few micrometres. Through a strain-gauge feedback, the accuracy of forces applied to both ends of the bender from two high-voltage piezoelectric actuators was within 0.03 N. The sample chamber was mounted on a granite support to isolate mechanical vibration, and equipped with kinematic mounts to adjust the chamber position and orientation. The top of the chamber contained a sample XYZ-manipulator on a rotating platform with differential pumping. An aperture located in vacuum before the sample set the bandwidth of the AGM. A commercial charge-coupled device (CCD) detector (1024  $\times$  1024 pixels, pixel resolution 13.5  $\mu\text{m}$ ) collected inelastically scattered X-rays under angle 70° of inclination. The AGS grating chamber and the CCD were independently positioned on granite slabs situated separately on two sliding platforms made of granite. Both the AGS grating chamber and the CCD can be lifted 30  $\mu\text{m}$  through an air-cushion mechanism such that the AGS can swing in the scattering plane to perform the measurements of momentum-resolved RIXS.

To test the energy-compensation principle, we used a carbon sample to measure the lineshape of elastically scattered X-rays. Both actuators of AGM and AGS benders were first optimized. The best

spectral resolution of the test AGM-AGS system was 108 meV at X-rays of energy 870 eV. The inset of Fig. 2 shows plots of scattering intensity versus photon energy with varied size of the sample aperture. The measured spectral resolution was insensitive to the aperture opening, as plotted in Fig. 2; the scattered intensity was nearly proportional to the aperture opening, agreeing satisfactorily with a prediction based on the energy-compensation principle. In particular, a large sample aperture, e.g. 400  $\mu\text{m}$ , does not smear the spectral resolution, in contrast to a SGM design. In addition, from our RIXS measurement of NiO,<sup>2</sup> although the bandwidth of the incident X-rays was large, we achieved a total energy of RIXS slightly better than that of data recorded using the ADDRESS<sup>3</sup> beamline and SAXES<sup>4</sup> spectrometer. This prominent feature is helpful to a *photon-hungry* experiment such as ultrahigh-resolution RIXS. Our experimental results demonstrate that the energy-compensation principle is effective for soft X-ray spectrometry, and greatly increases the measurement efficiency.

The commissioning results of the RIXS measurements concluded that the AGM-AGS scheme is an effective approach to improve the efficiency while maintaining great spectral resolution. We plan to establish an AGM-AGS system that comprises a polarization analyser at Taiwan Photon Source. The beamline is designed with an energy range from 400 eV to 1,200 eV. In addition, a new horizontal focusing mirror will be installed before the sample to decrease the horizontal beam size on the sample. A long exit arm of AGS will serve to decrease the limitation of the CCD pixel size and to increase the spectral resolution. AGS exit arms will be extended to 5 m (3.5 m in the present design of TLS) for an ultrahigh-resolution mode, in hope of achieving a resolution power greater than 40,000 at 900 eV. The construction plan of a new sample chamber is in progress to realize a continuous variation of momentum transfer without breaking the vacuum, allowing us to implement momentum-resolved RIXS measurements.

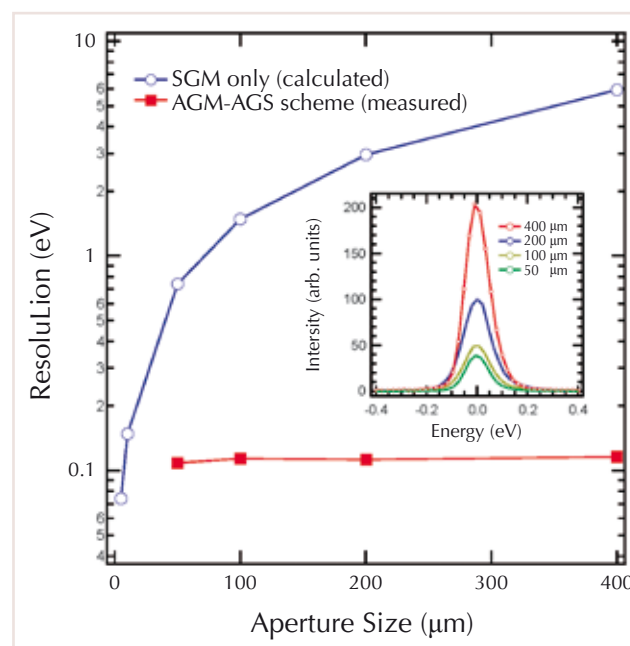


**Fig. 2:** Test of the energy-compensation principle. The FWHM of elastic scattering from a carbon sample is compared with that from a theoretical prediction based on the energy-compensation principle. Inset: lineshapes of elastic scattering of photons of energy 850 eV from a carbon sample with varied opening of the aperture.

## References

1. H. S. Fung, C. T. Chen, L. J. Huang, C. H. Chang, S. C. Chung, D. J. Wang, T. C. Tseng, and K. L. Tsang, AIP Conf. Proc. **705**, 655 (2004).
2. C. H. Lai, H. S. Fung, W. B. Wu, H. Y. Huang, H. W. Fu, S. W. Lin, S. W. Huang, C. C. Chiu, D. J. Wang, L. J. Huang, T. C. Tseng, S. C. Chung, C. T. Chen, and D. J. Huang, J. Synchrotron Rad. **21**, 325 (2014).
3. V. N. Strocov, T. Schmitt, U. Flechsig, T. Schmidt, A. Imhof, Q. Chen, J. Raabe, R. Betemps, D. Zimoch, J. Krempasky, X. Wang, M. Grioni, A. Piazzalunga, and L. Patthey, J. Synchrotron Rad. **17**, 6310643 (2010).
4. G. Ghiringheli, A. Piazzalunga, C. Dallera, G. Trezzi, L. Braicovich, T. Schmitt, V. N. Strocov, R. Betemps, L. Patthey, X. Wang, and M. Grioni, Rev. Sci. Instrum. **77**, 113108 (2006).